Journal of Magnetism and Magnetic Materials 497 (2020) 165998

Contents lists available at ScienceDirect

Journal of Magnetism and Magnetic Materials

journal homepage: www.elsevier.com/locate/jmmm

Research articles

Temperature dependent magneto-mechanical properties of magnetorheological elastomers

Qianqian Wen[a], Longjiang Shen[b], Jun Li[c], Shouhu Xuan[a], Zhiyuan Li[c], Xiwen Fan[a], Binshang Li[c], Xinglong Gong[a,*]

[a] CAS Key Laboratory of Mechanical Behavior and Design of Materials, Department of Modern Mechanics, CAS Center for Excellence in Complex System Mechanics, University of Science and Technology of China, Hefei 230027, Anhui, China
[b] Hunan Bogie Engineering Research Center, Zhuzhou 412000, Hunan, China
[c] Anhui Weiwei Rubber Parts Group Co.Ltd., Tongcheng 231400, Anhui, China

ARTICLE INFO

Keywords:
Temperature dependent
Magnetorheological elastomers
Particle movement
Magneto-mechanical

ABSTRACT

Temperature is one of the biggest influencing factors affecting the performance of polymer composites. The study on the temperature-dependent mechanical properties of magnetorheological (MR) elastomers is very necessary for its practical application. In this work, the dynamic and static mechanical properties of anisotropic MR elastomers were investigated under different temperatures. The results showed that both the initial modulus and the magnetic-induced modulus of MR elastomers decreased with increasing temperature. The variation of magnetic-induced modulus with temperature indicated the temperature-dependent rotation of particle chain inside the MR elastomers. The expression of magnetic-induced modulus as a function of the magnetic field and initial modulus was obtained by the theoretical analysis of the temperature-dependent rotation. It was found that when the magnetic field was constant, the reciprocal of the magnetic-induced modulus was linearly related to the reciprocal of the initial modulus at the corresponding temperature, which agreed well with the experimental result.

1. Introduction

Magnetorheological (MR) elastomers are one of MR materials family whose properties can be controlled quickly and reversibly by external magnetic fields [1–3]. MR elastomers are generally prepared by dispersing magnetic particles in non-magnetic elastomer matrix [4–9]. Compared with MR fluids, the solid matrix of MR elastomers can effectively overcome the problem in the applications of MR fluids, such as particle sedimentation, sealing issues, environmental contamination [10,11]. In addition, because of its large modulus changes and fast response time, the MR elastomers have attracted broad attention in semi-active vibration control [12–15], such as vibration isolator [16–19] and absorbers [20–22].

The matrixes of MR elastomers are typically a polymer such as silicone rubber [5,23–25], natural rubber [26–28], polyurethane [29,30], polydimethylsiloxane (PDMS) [6,31,32], and the temperature is one of the most influential factors affecting the performance of polymer materials. The devices based on MR elastomers often work in a wide range of temperatures. Therefore, it is important to study the effect of temperature on the mechanical properties of MR elastomers. Until now, there are a few research on the temperature-dependent performance of MR elastomers. Zhang *et al.* [33] evaluated the mechanical properties of MR elastomers based on a mixed rubber matrix (cis-polybutadiene rubber and natural rubber). The results revealed that the temperature-dependent moduli exhibited different characteristics for MR elastomers with different rubber matrices. Lejon *et al.* [34] conducted a measurement to study the influence of temperature, dynamic strain amplitude, magnetic field strength and frequency on the dynamic shear modulus of magnetosensitive (MS) elastomers. The measurements indicated that the temperature was the most influential on the parameters especially when the temperature reached the transition phase of the material. Wan *et al.* [35] found that the transition temperature of the MR elastomers appeared at about 50 °C, and the storage modulus initially decreased with the increase of temperature, reaching its minimum value at 50 °C and then started to increase with further increasing temperature.

However, previous studies on the temperature-dependent performance of MR elastomers are mainly concerned with the effect of temperature on the properties of the polymer matrix, and little attention is paid to the effect of temperature on the magneto-mechanical properties.

* Corresponding author.
E-mail address: gongxl@ustc.edu.cn (X. Gong).

https://doi.org/10.1016/j.jmmm.2019.165998
Received 17 May 2019; Received in revised form 6 October 2019; Accepted 16 October 2019
Available online 18 October 2019
0304-8853/ © 2019 Elsevier B.V. All rights reserved.

The change in modulus under an external magnetic field is the most distinctive rheological property of MR elastomers [12]. More importantly, the magneto-mechanical properties of MR elastomers are closely related to the arrangement of internal particles [1,36], and its changes can directly reflect the differences in the microscopic arrangement of internal particles. Therefore, to fully understand the temperature-dependent performance of MR elastomers, it is necessary to investigate the influence of temperature on the magneto-mechanical performance, which is helpful for their practical application and mechanism analysis.

In this study, the MR elastomers based on carbonyl iron particles and polydimethylsiloxane (PDMS) were prepared. The shear modulus of MR elastomers was investigated under different temperatures and different magnetic fields. The detailed mechanism was discussed and the comparison between the theory and experiment was conducted. A two-stage stress relaxation experiment at different temperature was conducted to further demonstrate the temperature-dependent rotation of particle chain inside the matrix

2. Material and methods

The MR elastomers were prepared from three raw materials: carbonyl iron (CI) particles, polydimethylsiloxane (PDMS) and curing agent. The CI particles (Type CN) have an average diameter of 6 μm, which are provided by BASF Co., Germany. The PDMS (Type Sylgard 184) and matching curing agent are provided by Dow Corning GmbH, USA. The preparation process of anisotropic MR elastomer samples mainly comprised three steps: Firstly, the three raw materials were uniformly mixed in a certain ratio. The mass fraction of carbonyl iron (CI) particles in this experiment was 70 wt% (volume fraction of 25 vol %). Secondly, this homogeneous mixture was placed in a vacuum chamber for 10 min to remove air bubbles inside the mixture. Finally, the mixture was cured at 90 °C for 20 min. At the same time of curing, a magnetic field of 1.5 T along the thickness direction of the sample was applied so that the carbonyl iron (CI) particles can form a chain-like structure inside anisotropic MR elastomers.

The magnetic properties of the MR elastomers at room temperature were measured by Hysteresis Measurement of Soft and Hard Magnetic Materials (HyMDC Metis, Leuven, Belgium). The shear modulus of MR elastomers at different temperatures and magnetic fields was measured by a plate-plate magneto-rheometer [37] (Physica MCR 302, Anton Paar, Austria). The sizes of the MR elastomer samples were approximately 20 mm in diameter and 1 mm in thickness. The applied test magnetic fields were parallel to the thickness direction of the sample, that is, the direction of the internal particle chain. The measurement of shear modulus was conducted at shear oscillation amplitude of 1%, frequency of 1 Hz, normal force of 10 N. The time interval of each test point was set to 10 s.

3. Results and discussion

3.1. The microstructure of MR elastomers

The microstructures of MR elastomer sample were observed by scanning electron microscopy (SEM) with an accelerating voltage of 15 kV. Fig. 1 presented SEM images of anisotropic MR elastomer with 70 wt% CI particles at different magnifications. The white round spots were the CI particles and the black background was the elastomer matrix. Because the samples were prepared under applying an external magnetic field, the CI particles showed obvious chain-like structure along the direction of the pre-structure magnetic field. It was noticed that the distance between adjacent particles on the same chain was very small.

3.2. The magnetic properties of CI particles in the MR elastomers

Fig. 2 showed the hysteresis loop of CI particles in the prepared MR elastomer sample at room temperature. It can be seen that CI particles exhibited a typical soft magnetic property, with a low coercive force, residual magnetization, and high saturation magnetization. For further quantitative analysis, the Langevin function, $M = aL(bH) = a[\coth(bH) - 1/(bH)]$, was used to approximate the magnetization of particles (M) under different magnetic fields (H), where a and b were fitting parameters. The fitted curve was shown by the blue line in Fig. 2, and its expression was given by:

$$M = 2000[\coth(0.023H) - 1/(0.023H)] \quad (1)$$

3.3. The temperature dependence of magnetic-induced modulus

Fig. 3a presented the shear storage modulus of MR elastomers as a function of the magnetic field at different temperatures. The results showed that the shear modulus of MR elastomers increased with increasing of the magnetic field and tended to be saturated at the high magnetic field. The property that modulus can be controlled by an external magnetic field is one of the typical properties of MR elastomers. On the other hand, as the temperature increased, the overall shear modulus was continuously decreasing. This can be seen more clearly from the initial storage modulus at different temperatures shown in Fig. 3c. As the temperature rose from 20 °C to 50 °C, the initial modulus dropped from 165.0 kPa to 78.8 kPa. This phenomenon can be explained by the temperature dependent rheological property of the MR elastomer matrix. The matrix of the MR elastomer is generally a high molecular polymer, such as silicone rubber, natural rubber, or PDMS used in this experiment. As the temperature increases, the increasing molecular chain thermal motion in the polymer will gradually overcome the interaction between the molecules. This will cause relative movement between the molecular chains, resulting in a continuous decrease in the overall modulus of the polymer.

Fig. 3b showed the magnetic-induced modulus as the function of the magnetic field at different temperatures. The magnetic-induced modulus is defined as the modulus of MR elastomers under a certain magnetic field minus the initial modulus under a zero magnetic field. Similar to the change in initial modulus, the magnetic-induced modulus also decreased with increasing temperature. When the temperature was 20 °C, the maximum magnetic-induced modulus was 99.5 kPa. When the temperature was raised to 50 °C, the maximum magnetic-induced modulus was reduced to 41.2 kPa. Fig. 3d showed the temperature dependence of the magnetic-induced modulus under different magnetic fields. In addition to the maximum magnetic-induced modulus, the magnetic-induced modulus at any certain magnetic field would decrease with increasing temperature. Moreover, the larger the external magnetic field, the greater the decrease in the magnetic-induced modulus as temperature increased. When the magnetic field was 70 kA/m, the magnetic-induced modulus decreased from 19.0 kPa to 8.7 kPa as the temperature rose from 20 °C to 50 °C, and the modulus decreased by 10.3 kPa. While the magnetic field rose to 490 kA/m, the magnetic modulus decreased from 97.2 kPa to 40.4 kPa, and the modulus decreased by 56.8 kPa, which was much higher than that at the magnetic field of 70 kA/m.

According to particle interaction-based models of MR elastomers [1,36,38], the magnetic-induced modulus is mainly determined by the magnetic properties of internal magnetic particles (such as the saturation magnetization) and the microstructure of the particles (such as the distance between the particles), but not related to the elastomer matrix. The internal particles of MR elastomers are generally considered to be immobilized in the matrix, and there is no particles movement relative to the matrix. This is one of the characteristics of MR elastomers compared with other MR materials. The previous particle interaction-based models are often based on this assumption so that only the

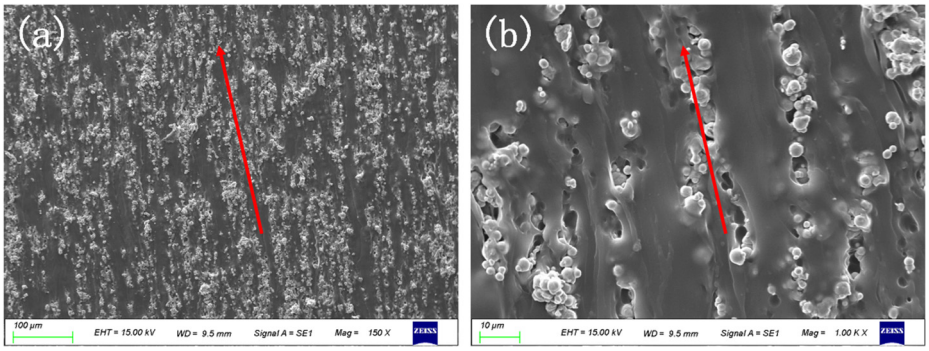

Fig. 1. SEM images of anisotropic MR elastomer with 70 wt% CI particles at (a) 150× magnification and (b) 1000× magnification. The red arrows indicated the direction of the particle chains. (For interpretation of the references to colour in this figure legend, the reader is referred to the web version of this article.)

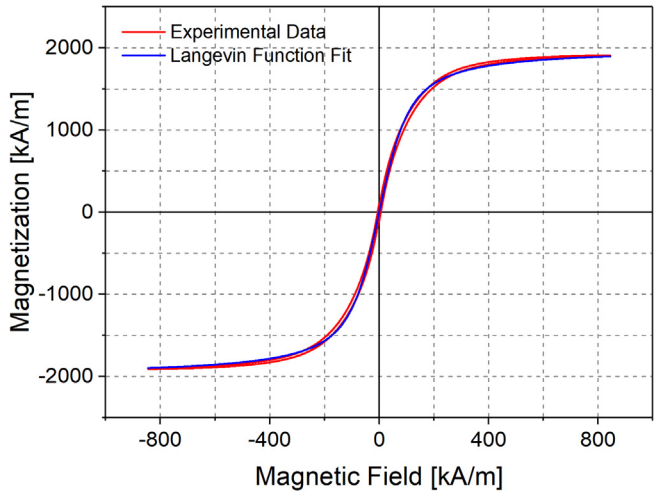

Fig. 2. Magnetic hysteresis loop of CI particles in the MR elastomer sample.

magnetic interaction between the particles is analyzed and the particles movement relative to the matrix is neglected. This assumption is reasonable when the modulus of MR elastomers is high. However, when the elastomer matrix exhibits a low modulus and the external magnetic field is relatively high, the particles' movement relative to the matrix cannot be ignored. The particle's movement has been reported in the previous studies on the magnetic properties of MR elastomers [39–41]. These studies showed that the particles were able to change their position within the MR elastomers under the influence of magnetic forces, resulting in a change of its magnetic properties. As shown in Fig. 3c, the temperature could cause a large change in the modulus of the polymer matrix. Therefore, it is necessary to consider the particles' movement within the polymer matrix when studying the effect of temperature on the performance of MR elastomers.

The MR elastomers generally work in a shear mode, and the schematic diagram of rotation of particles chains inside the matrix is shown in Fig. 4. When the magnetic field is zero ($H = 0$), there is no interaction force between the particles, and the particle chains will move along with the matrix and rotate the same angle. After the magnetic field is

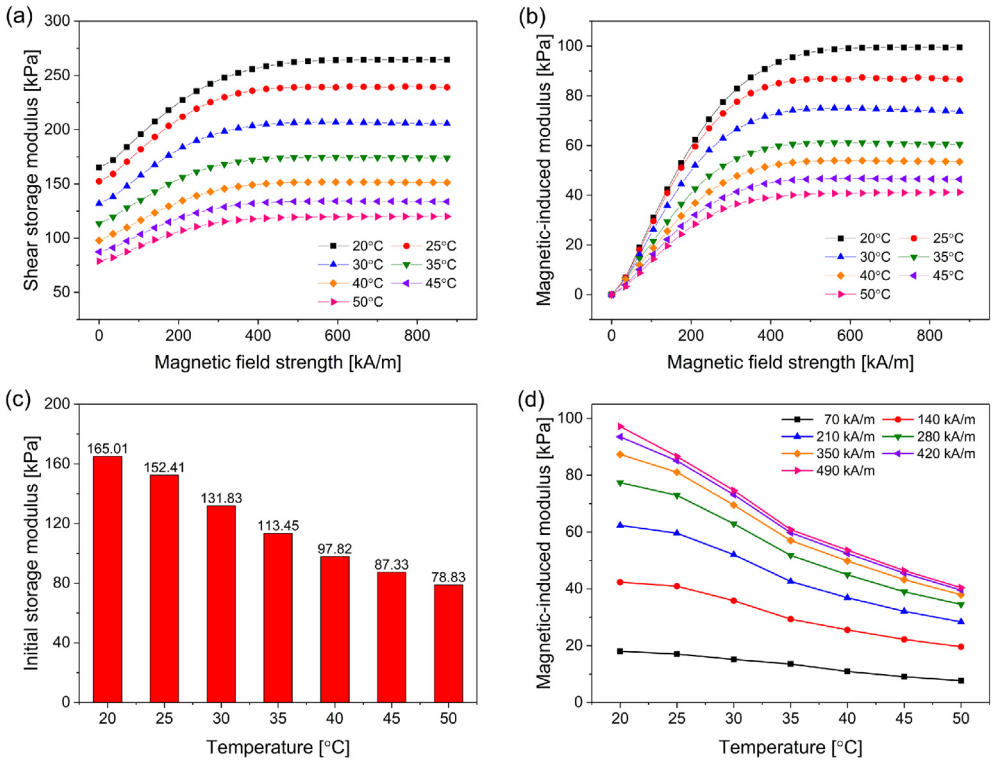

Fig. 3. The magnetic field dependence of (a) shear storage modulus and (b) magnetic-induced modulus at different temperatures. The temperature dependence of (c) initial storage modulus and (d) magnetic-induced modulus under different magnetic fields.

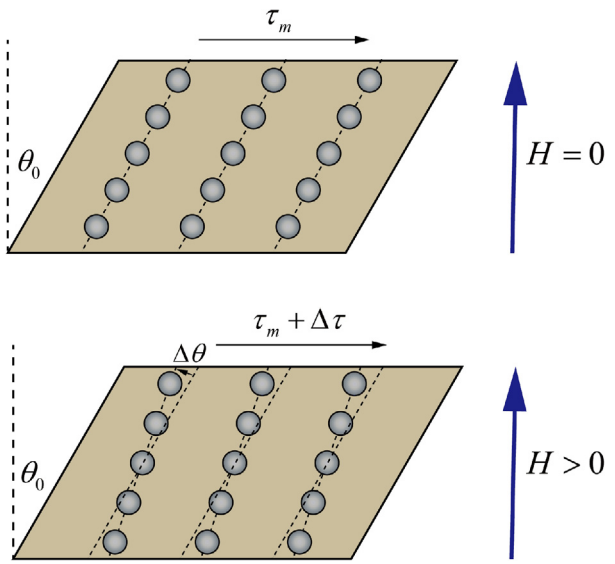

Fig. 4. Schematic diagram of the rotation of particles chains in the shear mode.

applied ($H > 0$), the particles are rapidly magnetized, and the magnetic interaction between the particles will cause the particle chains to turn to the external magnetic field. This rotation of the particle chains is hindered by the matrix and finally stopped at a certain equilibrium angle. This hindrance of the matrix can be characterized by the magnitude of its modulus. The higher the temperature, the smaller the hindrance of the polymer matrix, and the greater the rotation angle ($\Delta\theta$) of the particle chains. The increase of $\Delta\theta$ with increasing temperature results in a greater reduction in the magnetic-induced modulus (Fig. 3d).

3.4. Mechanism

To better illustrate the effect of temperature on the magnetic-induced modulus of MR elastomers, the rotation angle of the particle chains at different initial moduli can be obtained by analyzing the magnetic interaction between the particles and the interaction between the particle chains and the matrix. As shown in Fig. 5, it is assumed that the diameter and magnetic moment of individual particles is the same as d and m, respectively. The distance between the particles is the same

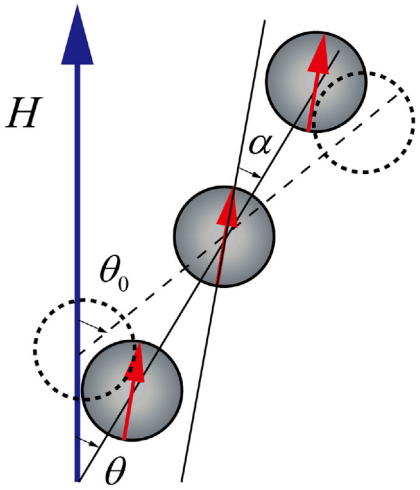

Fig. 5. Schematic diagram of the angles associated with the rotation of the particle chain. Red arrows represent the magnetic moment of individual particles. (For interpretation of the references to colour in this figure legend, the reader is referred to the web version of this article.)

as r. θ_0 is the angle between the particle chain and the direction of the external magnetic field before rotation of particle chains, and θ is the equilibrium angle after rotation. α is the angle between the moment and the particle chains at the equilibrium position.

For the particle chain containing N particles, the total magnetic dipole interaction energy E, and the relationship between θ and α are given by [42]:

$$E = \frac{0.6\mu_0 N m^2}{\pi r^3}(1 - 3\cos^2\alpha) \tag{2}$$

$$\frac{\sin 2\alpha}{\sin(\theta - \alpha)} = \frac{H}{0.3M} \tag{3}$$

where μ_0 is the vacuum permeability, H is the external magnetic field strength, and M is the magnetization of the individual particles. When the shear strain is small, $\sin 2\alpha \approx 2\alpha$, $\sin(\theta - \alpha) \approx \theta - \alpha$, Eq. (3) can be rewritten as

$$\alpha = \frac{1}{0.6M/H + 1}\cdot\theta = K_\chi\cdot\theta \tag{4}$$

The torque on the particle chain (T_p) caused by the magnetic interaction between the particles (the negative sign represents the counterclockwise direction):

$$T_p = -\frac{\partial E}{\partial\alpha} = -\frac{1.8\mu_0 N m^2}{\pi r^3}\sin 2\alpha \approx -\frac{3.6\mu_0 N m^2}{\pi r^3}\cdot\alpha = -K_m K_\chi\cdot\theta \tag{5}$$

which shows that the particle chain is rotated to the direction of the external magnetic field by T_p. With the rotation of the particle chain (that is, decreasing of θ), T_p decreased gradually.

On the other hand, the torque (clockwise) that hinders the rotation of the particle chain is given by:

$$T_m = G_m(\theta_0 - \theta)\cdot S\cdot D = \lambda G_0 V(\theta_0 - \theta) \tag{6}$$

where S and D are the thickness and bottom area of the MR elastomer sample, respectively, $V = D\cdot S$, is the volume of the sample, and $\lambda = G_m/G_0$, is the ratio of the matrix modulus (G_m) to the initial modulus of MR elastomer (G_0), generally $\lambda > 1$. The mechanical equilibrium, $T_m + T_p = 0$, gives the relationship between θ and θ_0:

$$\lambda G_0 V(\theta_0 - \theta) - K_m K_\chi\cdot\theta = 0 \tag{7}$$

$$\theta = \frac{\lambda G_0 V}{\lambda G_0 V + K_m K_\chi}\cdot\theta_0 = \frac{1}{1 + K_m K_\chi/\lambda G_0 V}\cdot\theta_0 \tag{8}$$

which indicates that θ decreases with the decrease of G_0 when the magnetic field is constant. In other words, the rotation angle $\Delta\theta$ ($=\theta_0 - \theta$) will become larger as G_0 decreases.

The increase in shear stress ($\Delta\tau$ in Fig. 4) caused by torque on the particle chains (T_P) is:

$$\Delta\tau = \frac{T_P}{S\cdot D} = \frac{T_P}{V} \tag{9}$$

Thus, the magnetic-induced modulus (ΔG) is given by:

$$\Delta G = \frac{\Delta\tau}{\theta_0} = \frac{T_P}{V\theta_0} = \frac{\lambda K_m K_\chi G_0}{\lambda G_0 V + K_m K_\chi} \tag{10}$$

$$\frac{1}{\Delta G} = \frac{1}{\lambda G_0} + \frac{1}{K_\chi\cdot K_m/V} \tag{11}$$

According to the relationship between magnetic moment and magnetization, $m = M\cdot V_P$, where $V_P = 1/6\pi d^3$ is the volume of individual particles, the parameters K_m/V in Eq. (11) can be expressed as:

$$\frac{K_m}{V} = \frac{3.6\mu_0 N m^2}{\pi r^3 V} = \frac{3.6\mu_0 N(MV_p)^2}{\pi r^3 V} = 0.6\mu_0 M^2\cdot\frac{NV_P}{V}\cdot\frac{V_P}{1/6\cdot\pi r^3} = \frac{0.6\mu_0 M^2 C}{n^3} \tag{12}$$

where $C = NV_P/V$ is the volume fraction of the particles, and $n = r/d$ is

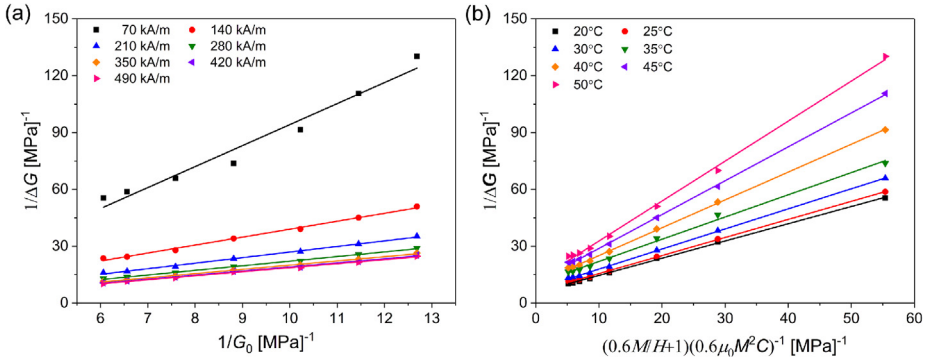

Fig. 6. (a) Linear correlation between $1/\Delta G$ and $1/G_0$ under different magnetic field. (b) Linear correlation between $1/\Delta G$ and $(0.6M/H + 1)/(0.6\mu_0 M^2 C)$ at different temperatures. The solid points represent experimental data, and the straight lines are linear fitting curves.

the ratio of the distance between the particles to the diameter of the particles, and generally $n > 1$.

In summary, the magnetic-induced modulus of MR elastomers as the function of the initial modulus and the magnetic field strength can be given by (4), (11) and (12) as follows:

$$\frac{1}{\Delta G} = \frac{1}{\lambda}\cdot\frac{1}{G_0} + n^3\cdot\frac{0.6M/H + 1}{0.6\mu_0 M^2 C} \tag{13}$$

The relationship between M and H is determined by the magnetization properties of the particles as shown in Eq. (1). It can be seen from Eq. (13) that when the temperature is constant (that is, G_0 is constant), $1/\Delta G$ is linearly related to $(0.6M/H + 1)(0.6\mu_0 M^2 C)^{-1}$, and the slope is n^3. When the magnetic field strength is constant, $1/\Delta G$ is linearly related to $1/G_0$, and the slope is $1/\lambda$. Both linear correlations can be confirmed by experimental data, as shown in Fig. 6.

3.5. The time dependence of shear stress at different temperatures

In order to show the temperature-dependent rotation of particle chain inside the matrix more clearly, a two-stage shear relaxation experiment (Fig. 7a) was carried out. The first stage of the experiment ($0 \le t < 300s$) was a shear stress relaxation experiment of MR elastomers at zero magnetic field: a constant shear strain, $\gamma_0 = 1\%$, was applied at $t = 0$. Because there was no magnetic field interaction, the shear stress in the first stage (τ_1) was equal to the relaxation stress of the matrix (τ_{m1}), that is, $\tau_1(t) = \tau_{m1}(t)$. The second stage of the experiment ($t \ge 300s$) was the shear stress relaxation experiment under a step magnetic field: the shear strain was kept constant at $\gamma_0 = 1\%$ and a step magnetic field, $H = 525\ kA/m$, was applied at $t = 300s$. The shear stress in the second stage (τ_2) consists of relaxation stress of the matrix (τ_{m2}) and magnetic-induced shear stress ($\Delta\tau$). Because the shear strain was kept the same in the two stages, τ_{m2} is considered to have the same expression with τ_{m1}, that is, $\tau_{m2}(t) = \tau_{m1}(t) = \tau_m(t)$.

Fig. 7b presented the time dependence of shear stress at different temperatures in the two-stage shear relaxation experiment. In the first stage ($0 \le t < 300s$), the change of τ_1 with time exhibited the typical stress relaxation behavior of viscoelastic materials: under constant shear strain, the shear stress of the materials decreased with time and tended to a certain constant value. Viscoelasticity is one of the main mechanical characteristics of the polymer matrix. Moreover, τ_1 at higher temperature was overall smaller than that at lower temperature, indicating that the relaxation modulus of MR elastomers decreased with increasing temperature. It agreed well with the trend of the initial storage modulus with temperature (Fig. 3c).

In the second stage ($t \ge 300s$), the magnetic-induced shear stress ($\Delta\tau$) at different temperatures could be obtained by

$$\Delta\tau(t) = \tau_2(t) - \tau_m(t) \tag{14}$$

$\tau_m(t)$ in the second stage could be predicted from the fitted Prony series of $\tau_1(t)$. The Prony series is a commonly used fitting function in the viscoelastic analysis. It can be expressed as:

$$\tau(t) = A_0 + \sum_{n=1}^{N} A_n e^{-t/t_n} \tag{15}$$

where A_n and t_n are the amplitude and the characteristic time of the n-th series item, respectively. As shown in Fig. 7b, taking the temperature of 20 °C as an example, τ_{m20} was the fitted relaxation stress of the matrix by the Prony series ($N = 4$), and $\Delta\tau_{20}$ was the magnetic-induced shear stress in the second stage. The $\Delta\tau$ at other temperatures could be obtained in the same way.

Fig. 8 showed the time dependence of the magnetic-induced shear stress ($\Delta\tau$) at three different temperatures. It can be seen that $\Delta\tau$ rose rapidly after applying the magnetic field. It was attributed to the rapid magnetization of the soft magnetic particles under the magnetic field. After a rapid rise, $\Delta\tau$ gradually decreased with time. This could reflect the rotation of the particle chain inside the matrix. From Eq. (5), driven by the torque on the particle chain (T_p) caused by the magnetic interaction between the particles, the particle chain was rotated to the direction of the external magnetic field as shown in Fig. 4. With the rotation of the particle chain (that is, decreasing of θ), T_p decreased gradually, resulting in the decrease in $\Delta\tau$ over time. Moreover, Fig. 8 showed that $\Delta\tau$ at the higher temperature was generally smaller. It could be explained by the lower modulus of matrix at higher temperature. A lower modulus of polymer matrix represented the smaller hindrance to the rotation of particle chain, resulting in the larger rotation angle ($\Delta\theta$) and smaller equilibrium angle (θ) of the particle chain. From Eqs. (8) and (9), $\Delta\tau$ would be smaller because of the smaller θ at higher temperature.

Furthermore, it could be predicted from Fig. 8 that $\Delta\tau$ would gradually stabilize and tend to a certain value, which corresponded to the equilibrium position of the particle chain's rotation. Because of the viscoelastic properties of the polymer matrix, the process that $\Delta\tau$ reached the steady state in the second stage was not instantaneous, but time-dependent. The time-dependent $\Delta\tau$ indicated that it took time for the particle chain to move to the equilibrium position after applying an external magnetic field. It should be noted from Fig. 8 that $\Delta\tau$ at higher temperatures reached the steady state more quickly. This was because the increase in temperature accelerated the rate of molecular motion of polymer matrix, resulting in a shorter time for one equilibrium state of the molecule to another equilibrium state. In the measurement of the storage modulus at different magnetic fields and temperatures, the test point interval was set to 10 s so the intermediate process of particles movement was ignored in the previous analysis, and only the equilibrium state was considered. Nevertheless, when the MR elastomers are subjected to a fast changing magnetic field, further studies on this time-related particle movement are also necessary in the future research.

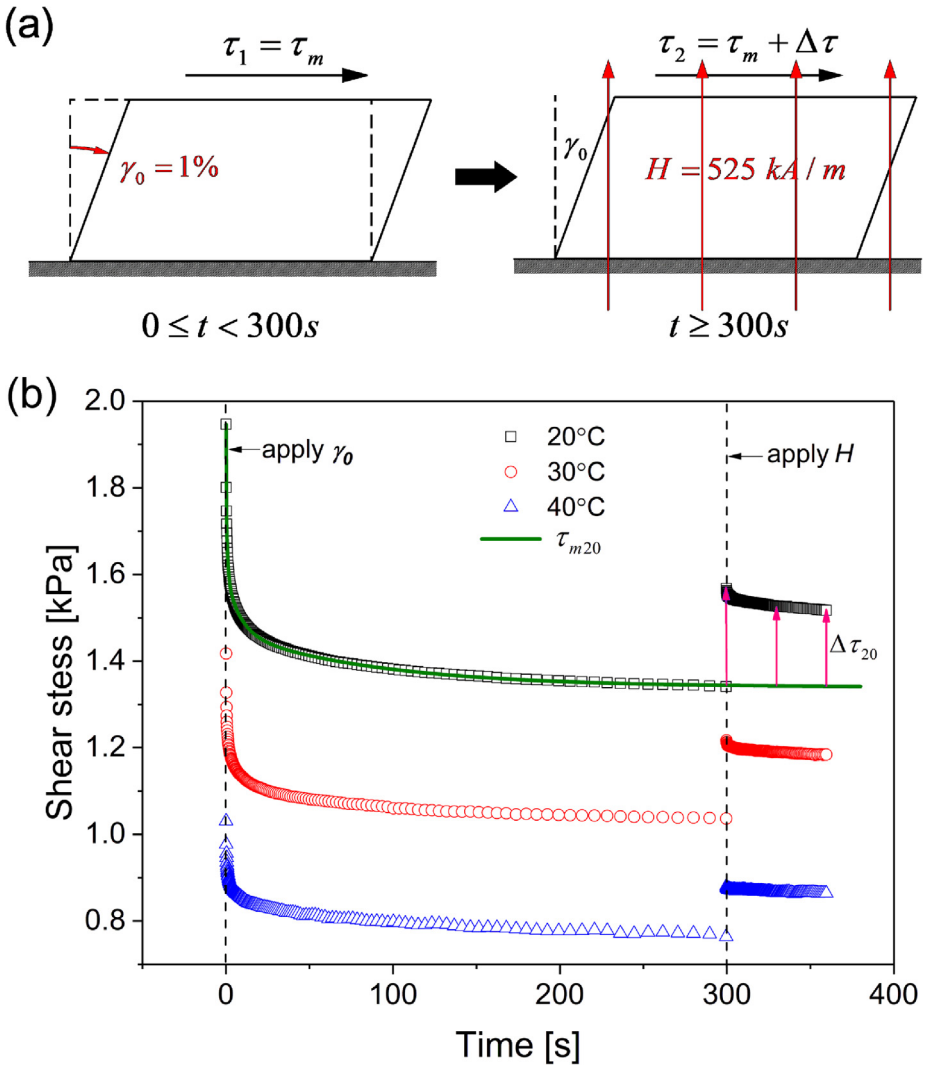

Fig. 7. (a) The two-stage shear relaxation experiment. (b) The time dependence of shear stress at different temperatures in the two-stage experiment.

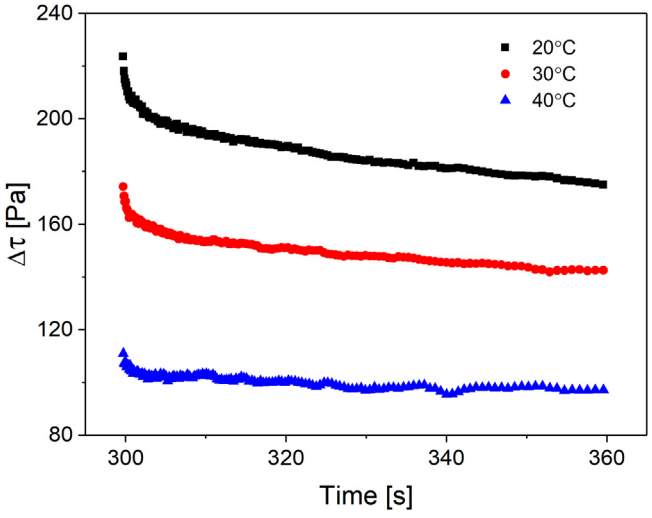

Fig. 8. The time dependence of magnetic-induced shear stress ($\Delta\tau$) at different temperature.

4. Conclusions

In this study, the influence of temperature on the magneto-mechanical properties of MR elastomers was investigated. The results showed that both the initial modulus and magnetic-induced modulus decreased with increasing temperature. As the temperature rose from 20 °C to 50 °C, the initial modulus decreased from 165.0 kPa to 78.8 kPa, and the maximum magnetic-induced modulus decreased from 99.5 kPa to 41.2 kPa. The decrease in the magnetic-induced modulus was caused by the rotation of the particle chains inside the elastomer matrix.

By analyzing the magnetic interaction between the particles and the action of the particle chain and the matrix, the relationship between the magnetic-induced modulus and the initial modulus at the corresponding temperature was obtained. The expression showed that the reciprocal of the magnetic-induced modulus was linearly related to the reciprocal of the initial modulus when the applied magnetic field was constant. This relationship was proved by the experimental results. The two-stage stress relaxation experiments at different temperatures were conducted. The changes of shear stress over time further demonstrated the temperature-dependent rotation of particle chain inside the matrix.

Declaration of Competing Interest

The authors declare that they have no known competing financial interests or personal relationships that could have appeared to influence the work reported in this paper.

Acknowledgments

Financial supports from the National Natural Science Foundation of China (Grant No. 11572309, 11822209, 11972343), the Strategic Priority Research Program of the Chinese Academy of Sciences (Grant No. XDB22040502), and the National Key R&D Program of China (Grant No. 2018YFB1201703) are gratefully acknowledged. This work is also supported by the Collaborative Innovation Center of Suzhou Nano Science and Technology.

References

[1] M.R. Jolly, J.D. Carlson, B.C. Munoz, A model of the behaviour of magnetorheological materials, Smart Mater. Struct. 5 (1996) 607–614, https://doi.org/10.1088/0964-1726/5/5/009.
[2] J.D. Carlson, M.R. Jolly, MR fluid, foam and elastomer devices, Mechatronics 10 (2000) 555–569, https://doi.org/10.1016/S0957-4158(99)00064-1.
[3] Z. Rigbi, L. Jilken, The response of an elastomer filled with soft ferrite to mechanical and magnetic influences, J. Magn. Magn. Mater. 37 (1983) 267–276, https://doi.org/10.1016/0304-8853(83)90055-0.
[4] M. Farshad, A. Benine, Magnetoactive elastomer composites, Polym. Test. 23 (2004) 347–353, https://doi.org/10.1016/S0142-9418(03)00103-X.
[5] X.L. Gong, X.Z. Zhang, P.Q. Zhang, Fabrication and characterization of isotropic magnetorheological elastomers, Polym. Test. 24 (2005) 669–676, https://doi.org/10.1016/j.polymertesting.2005.03.015.
[6] W.H. Li, M. Nakano, Fabrication and characterization of PDMS based magnetorheological elastomers, Smart Mater. Struct. 22 (2013) 055035, , https://doi.org/10.1088/0964-1726/22/5/055035.
[7] T.F. Tian, M. Nakano, Fabrication and characterisation of anisotropic magnetorheological elastomer with 45 degrees iron particle alignment at various silicone oil concentrations, J. Intell. Mater. Syst. Struct. 29 (2018) 151–159, https://doi.org/10.1177/1045389x17704071.
[8] S.A.A. Aziz, Ubaidillah, S.A. Mazlan, N.I.N. Ismail, S.B. Choi, Implementation of functionalized multiwall carbon nanotubes on magnetorheological elastomer, J. Mater. Sci. 53 (2018) 10122–10134, https://doi.org/10.1007/s10853-018-2315-3.
[9] U.R. Poojary, S. Hegde, K.V. Gangadharan, Experimental investigation on the effect of carbon nanotube additive on the field-induced viscoelastic properties of magnetorheological elastomer, J. Mater. Sci. 53 (2018) 4229–4241, https://doi.org/10.1007/s10853-017-1883-y.
[10] M. Ashtiani, S.H. Hashemabadi, A. Ghaffari, A review on the magnetorheological fluid preparation and stabilization, J. Magn. Magn. Mater. 374 (2015) 716–730, https://doi.org/10.1016/j.jmmm.2014.09.020.
[11] J. de Vicente, D.J. Klingenberg, R. Hidalgo-Alvarez, Magnetorheological fluids: a review, Soft Matter 7 (2011) 3701–3710, https://doi.org/10.1039/c0sm01221a.
[12] Y.C. Li, J.C. Li, W.H. Li, H.P. Du, A state-of-the-art review on magnetorheological elastomer devices, Smart Mater. Struct. 23 (2014) 123001, , https://doi.org/10.1088/0964-1726/23/12/123001.
[13] H. Deng, Y. Du, Z. Wang, J. Ye, J. Zhang, M. Ma, X. Zhong, Poly-stable energy harvesting based on synergetic multistable vibration, Commun. Phys. 2 (2019) 21, https://doi.org/10.1038/s42005-019-0117-9.
[14] V.S. Molchanov, G.V. Stepanov, V.G. Vasiliev, E.Y. Kramarenko, A.R. Khokhlov, Z.D. Xu, Y.Q. Guo, Viscoelastic properties of magnetorheological elastomers for damping applications, Macromol. Mater. Eng. 299 (2014) 1116–1125, https://doi.org/10.1002/mame.201300458.
[15] S.B. Choi, W.H. Li, M. Yu, H.P. Du, J. Fu, P.X. Do, State of the art of control schemes for smart systems featuring magneto-rheological materials, Smart Mater. Struct. 25 (2016) 043001, , https://doi.org/10.1088/0964-1726/25/4/043001.
[16] S. Opie, W. Yim, Design and control of a real-time variable stiffness vibration isolator, J. Intell. Mater. Syst. Struct. 22 (2011) 113–125, https://doi.org/10.1177/1045389x10389204.
[17] W.H. Li, X.Z. Zhang, H.P. Du, Development and simulation evaluation of a magnetorheological elastomer isolator for seat vibration control, J. Intell. Mater. Syst. Struct. 23 (2012) 1041–1048, https://doi.org/10.1177/1045389x11435431.
[18] Y.C. Li, J.C. Li, W.H. Li, B. Samali, Development and characterization of a magnetorheological elastomer based adaptive seismic isolator, Smart Mater. Struct. 22 (2013) 035005, , https://doi.org/10.1088/0964-1726/22/3/035005.
[19] H.F. Shi, M. Yu, M. Zhu, J. Fu, S.B. Choi, Z.W. Xing, An investigation of the dynamic behaviors of an MRE isolator subjected to constant and alternating currents, Smart Mater. Struct. 25 (2016) 077002, , https://doi.org/10.1088/0964-1726/25/7/077002.
[20] A.A. Lerner, K.A. Cunefare, Performance of MRE-based vibration absorbers, J. Intell. Mater. Syst. Struct. 19 (2008) 551–563, https://doi.org/10.1177/1045389x07077850.
[21] S.S. Sun, H.X. Deng, J. Yang, W.H. Li, H.P. Du, G. Alici, M. Nakano, An adaptive tuned vibration absorber based on multilayered MR elastomers, Smart Mater. Struct. 24 (2015) 045045, , https://doi.org/10.1088/0964-1726/24/4/045045.
[22] S.S. Sun, H.X. Deng, J. Yang, W.H. Li, H.P. Du, G. Alici, Performance evaluation and comparison of magnetorheological elastomer absorbers working in shear and squeeze modes, J. Intell. Mater. Syst. Struct. 26 (2015) 1757–1763, https://doi.org/10.1177/1045389x14568819.
[23] W.H. Li, Y. Zhou, T.F. Tian, Viscoelastic properties of MR elastomers under harmonic loading, Rheol. Acta 49 (2010) 733–740, https://doi.org/10.1007/s00397-010-0446-9.
[24] Y. Tong, X.F. Dong, M. Qi, Improved tunable range of the field-induced storage modulus by using flower-like particles as the active phase of magnetorheological elastomers, Soft Matter 14 (2018) 3504–3509, https://doi.org/10.1039/c8sm00359a.
[25] V.V. Sorokin, G.V. Stepanov, M. Shamonin, G.J. Monkman, A.R. Khokhlov, E.Y. Kramarenko, Hysteresis of the viscoelastic properties and the normal force in magnetically and mechanically soft magnetoactive elastomers: effects of filler composition, strain amplitude and magnetic field, Polymer 76 (2015) 191–202, https://doi.org/10.1016/j.polymer.2015.08.040.
[26] L. Chen, X.L. Gong, W.Q. Jiang, J.J. Yao, H.X. Deng, W.H. Li, Investigation on magnetorheological elastomers based on natural rubber, J. Mater. Sci. 42 (2007) 5483–5489, https://doi.org/10.1007/s10853-006-0975-x.
[27] H.S. Jung, S.H. Kwon, H.J. Choi, J.H. Jung, Y.G. Kim, Magnetic carbonyl iron/natural rubber composite elastomer and its magnetorheology, Compos. Struct. 136 (2016) 106–112, https://doi.org/10.1016/j.compstruct.2015.10.008.
[28] J.S. An, S.H. Kwon, H.J. Choi, J.H. Jung, Y.G. Kim, Modified silane-coated carbonyl iron/natural rubber composite elastomer and its magnetorheological performance, Compos. Struct. 160 (2017) 1020–1026, https://doi.org/10.1016/j.compstruct.2016.10.128.
[29] Y. Hu, Y.L. Wang, X.L. Gong, X.Q. Gong, X.Z. Zhang, W.Q. Jiang, P.Q. Zhang, Z.Y. Chen, New magnetorheological elastomers based on polyurethane/Si-rubber hybrid, Polym. Test. 24 (2005) 324–329, https://doi.org/10.1016/j.polymertesting.2004.11.003.
[30] M. Yu, S. Qi, J. Fu, M. Zhu, A high-damping magnetorheological elastomer with bi-directional magnetic-control modulus for potential application in seismology, Appl. Phys. Lett. 107 (2015) 111901, , https://doi.org/10.1063/1.4931127.
[31] I.A. Perales-Martinez, L.M. Palacios-Pineda, L.M. Lozano-Sanchez, O. Martinez-Romero, J.G. Puente-Cordova, A. Elias-Zuniga, Enhancement of a magnetorheological PDMS elastomer with carbonyl iron particles, Polym. Test. 57 (2017) 78–86, https://doi.org/10.1016/j.polymertesting.2016.10.029.
[32] T. Hu, S.H. Xuan, L. Ding, X.L. Gong, Stretchable and magneto-sensitive strain sensor based on silver nanowire-polyurethane sponge enhanced magnetorheological elastomer, Mater. Des 156 (2018) 528–537, https://doi.org/10.1016/j.matdes.2018.07.024.
[33] W. Zhang, X.L. Gong, S.H. Xuan, W.Q. Jiang, Temperature-dependent mechanical properties and model of magnetorheological elastomers, Ind. Eng. Chem. Res. 50 (2011) 6704–6712, https://doi.org/10.1021/ie200386x.
[34] J. Lejon, L. Kari, Measurements on the temperature, dynamic strain amplitude and magnetic field strength dependence of the dynamic shear modulus of magneto-sensitive elastomers in a wide frequency range, J. Vib. Acoust 135 (2013) 064506, , https://doi.org/10.1115/1.4025063.
[35] Y.X. Wan, Y.P. Xiong, S.M. Zhang, Temperature dependent dynamic mechanical properties of magnetorheological elastomers: experiment and modeling, Compos. Struct. 202 (2018) 768–773, https://doi.org/10.1016/j.compstruct.2018.04.010.
[36] Y. Shen, M.F. Golnaraghi, G.R. Heppler, Experimental research and modeling of magnetorheological elastomers, J. Intell. Mater. Syst. Struct. 15 (2004) 27–35, https://doi.org/10.1177/1045389x04039264.
[37] Q.Q. Wen, Y. Wang, X.L. Gong, The magnetic field dependent dynamic properties of magnetorheological elastomers based on hard magnetic particles, Smart Mater. Struct. 26 (2017) 075012, , https://doi.org/10.1088/1361-665X/aa7396.
[38] M.A. Cantera, M. Behrooz, R.F. Gibson, F. Gordaninejad, Modeling of magneto-mechanical response of magnetorheological elastomers (MRE) and MRE-based systems: a review, Smart Mater. Struct. 26 (2017) 023001, , https://doi.org/10.1088/1361-665X/aa549c.
[39] G.V. Stepanov, D.Y. Borin, Y.L. Raikher, P.V. Melenev, N.S. Perov, Motion of ferroparticles inside the polymeric matrix in magnetoactive elastomers, J. Phys.: Condens. Matter 20 (2008), https://doi.org/10.1088/0953-8984/20/20/204121.
[40] A.V. Bodnaruk, A. Brunhuber, V.M. Kalita, M.M. Kulyk, A.A. Snarskii, A.F. Lozenko, S.M. Ryabchenko, M. Shamonin, Temperature-dependent magnetic properties of a magnetoactive elastomer: immobilization of the soft-magnetic filler, J. Appl. Phys. 123 (2018) 115118, , https://doi.org/10.1063/1.5023891.
[41] A.V. Bodnaruk, V.M. Kalita, M.M. Kulyk, A.F. Lozenko, S.M. Ryabchenko, A.A. Snarskii, A. Brunhuber, M. Shamonin, Temperature blocking and magnetization of magnetoactive elastomers, J. Magn. Magn. Mater. 471 (2019) 464–467, https://doi.org/10.1016/j.jmmm.2018.10.005.
[42] S.R. Mishra, M.D. Dickey, O.D. Velev, J.B. Tracy, Selective and directional actuation of elastomer films using chained magnetic nanoparticles, Nanoscale 8 (2016) 1309–1313, https://doi.org/10.1039/c5nr07410j.